

NASA TT F-10,052

AN ANALOG EXPERIMENT ON TURBULENT LIQUID METAL HEAT
TRANSFER IN THE ENTRANCE REGION OF NONCIRCULAR DUCTS

J. T. Pearson and T. F. Irvine

FACILITY FORM 802	N66-235 44	
	(ACCESSION NUMBER)	(THRU)
	19	1
	(PAGES)	(CODE)
	33	(CATEGORY)
(NASA CR OR TMX OR AD NUMBER)		

Translation of "Model'noye issledovaniye
turbulentnogo teploobmena zhidkikh metallov vo vkhodnoy
oblasti trub nekruglogo secheniya."
Inzhenerno-Fizicheskiy Zhurnal, Vol. 6,
No. 6, pp. 10-19, 1963.

GPO PRICE \$ _____

CFSTI PRICE(S) \$ _____

Hard copy (HC) 1.00Microfiche (MF) .50

ff 653 July 65

NATIONAL AERONAUTICS AND SPACE ADMINISTRATION
WASHINGTON MARCH 1966

AN ANALOG EXPERIMENT ON TURBULENT LIQUID METAL HEAT
TRANSFER IN THE ENTRANCE REGION OF NONCIRCULAR DUCTS*10**

ABSTRACT

2 3544

An electrical analog made of conducting paper, electrical sheet, and metal foil is used to solve the two-dimensional Fourier equations. The analog was used to find the temperature distribution on the entrance walls for the case of a steady "creeping" flow in the entrance region of ducts with variously shaped noncircular cross sections.

It is necessary in many present-day heat exchangers, in order to reduce their size and weight, to use ducts with a noncircular cross section. Often the length of the duct is so short that the temperature and velocity profiles do not have a chance to become fully developed before the fluid has emerged from the tube. Consequently, in many compact heat exchangers the thermal and fluid entrance region occupies a considerable fraction of the duct length.

For a fully developed turbulent flow of liquid metal in circular ducts, Lyon (ref. 1), Clayborne (ref. 2), and others have ascertained that the heat transfer characteristics may be calculated by means of a suitable combination of individual factors due to molecular conduction and turbulent exchange. Inasmuch as the velocity profile in a turbulent flow approximates the profile of a slow flow, the convective heat transfer may be calculated from the magnitude of the molecular conductivity on the basis of the energy equation, wherein the real boundary conditions assuming a constant velocity distribution are used.

*Translated (into Russian) by E. A. Bogacheva.

**Numbers in the margin indicate pagination in the original foreign text.

Hartnett and Irvine (ref. 3) have used this method to analyze heat transfer in noncircular ducts. Also investigated in this paper were the various boundary conditions that could exist in the investigation of heat transfer in noncircular tubes. They indicated, in particular, that if the heat flux is given, one should be primarily concerned with the peripheral temperature distribution at the wall, since the structure of the flow usually requires the maximum working temperature possible. Consequently, the wall temperature distribution determined in the analysis of the slow flow problem may be taken as a limiting case in turbulent flow. Any turbulent transport will have a smoothing influence on the temperature distribution of creeping flow.

The objective of the present article is to investigate these creeping flow temperature distributions in the entrance region of ducts with various types of noncircular cross sections. These temperature distributions represent limiting¹¹ cases, but they may be used to build simplified constructions approximating the actual design conditions for small Re numbers in turbulent flow.

It is also instructive to note that the problem of convection of a steady creeping flow is at once the problem of heat conduction of a nonsteady flow for the case of a plane solid of the same cross section and under identical boundary conditions. The solutions given in the present article for all cross section configurations, with the exception of parallel plates and circles, have never been derived before.

INITIAL EQUATIONS AND ELECTRICAL SIMULATION PRINCIPLES

Consider the entrance region of a duct with a constant cross section (fig. 1a). Fluid enters the duct at a constant temperature T_0 , flowing through the duct at a constant velocity w . The coordinate system is chosen so that the z -axis will pass through the center of the duct cross section, the origin being

located at the duct entrance. With constant thermophysical characteristics on the part of the fluid in an incompressible flow, only an inconsequential viscous dissipation of energy, and low thermal conductivity in the axial direction, the heat conduction equation for a steady-state flow may be written as follows:

$$\frac{\partial^2 T}{\partial x^2} + \frac{\partial^2 T}{\partial y^2} = \frac{w}{a} \frac{\partial T}{\partial z}. \quad (1)$$

For a constant heat flux, the boundary conditions for Eq. (1) at the surface σ are the following

$$\begin{aligned} \frac{\partial T}{\partial n} &= -\frac{q_w}{k} = \text{const}, \\ T(x, y, 0) &= T_0 = \text{const}. \end{aligned} \quad (2)-(3)$$

With the dimensionless variables $\theta = \frac{T - T_0}{4q_w d_h / k}$, $Z = \frac{z}{d_h \text{RePr}}$, $X = \frac{x}{d_h}$, $Y = \frac{y}{d_h}$,

$N = \frac{n}{d_h}$, equation (1) and its associated boundary conditions are reduced to

dimensionless form. Equation (1) becomes

$$\frac{\partial^2 \theta}{\partial X^2} + \frac{\partial^2 \theta}{\partial Y^2} = \frac{\partial \theta}{\partial Z}, \quad (4)$$

and the boundary conditions (2) and (3) at the surface Σ are as follows:

$$\begin{aligned} \frac{\partial \theta}{\partial N} &= -\frac{1}{4}, \\ \theta(X, Y, 0) &= 0. \end{aligned} \quad (5)-(6)$$

The reduced temperature of the fluid is determined by the heat balance equation for an element of fluid:

$$dT_b = \frac{q_w P}{w A \rho c} dz. \quad (7)$$

Integrating from $T_b = T_0$, $z = 0$ to $T_b = T_b$, $z = z$, we obtain

12

$$\int_{T_0}^{T_b} dT = \int_0^z \frac{q_w P}{w A \rho c} dz. \quad (8)-(9)$$

$$T_b = T_0 + \frac{4q_w a z}{w k d_h}.$$

Reducing it to dimensionless form, we obtain

$$\theta_b = Z. \quad (10)$$

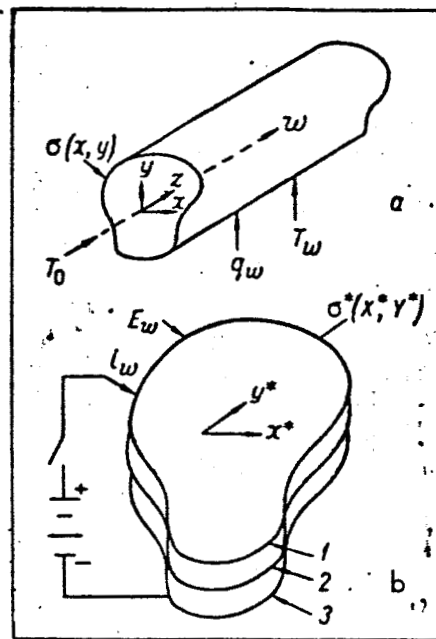


Figure 1. Diagram of Noncircular Duct (a) and Electrical Analog Model (b):
1) Conducting Sheet; 2) Dielectric; 3) Metal Foil.

Let us now examine an electrical model (ref. 4) consisting of a thin dielectric sheet placed between electrically conducting steel sheet and a sheet of metal foil (Fig. 1b). The boundary of the model is the curve $\sigma^* = \sigma^*(x^*, y^*)$, the form of which is the same as the duct cross section $\sigma(x, y)$. The coordinate system (x^*, y^*) is oriented such that the origin is located at the center of the curve σ^* , the x^*y^* -plane coinciding with the plane of the model. Electric current can flow in the model via the curve σ^* , and the

electrical circuit is closed by grounding the metal foil. If the resistance of the conducting sheet and the thickness of the dielectric are uniform over the entire model, the initial differential equation becomes

$$\frac{\partial^2 E}{\partial x^{*2}} + \frac{\partial^2 E}{\partial y^{*2}} = RC \frac{\partial E}{\partial t} \quad (11)$$

If after the passage of a certain time $t = 0$ the electric current flowing in the model is constant over a unit length of the curve σ^* and if the entire model is subjected to a uniform potential E until the time $t = 0$, the boundary conditions of equation (11) at the surface σ^* will be as follows:

$$\left. \begin{aligned} \frac{\partial E}{\partial n^*} &= -Ri_w = \text{const}, \\ E(x^*, y^*, 0) &= E_0 = \text{const}. \end{aligned} \right\} \quad (12)-(13)$$

These equations reduce to normal form with a suitable choice of the following dimensionless variables: $\theta^* = \frac{E - E_0}{4i_w d_h^2 R}$, $z^* = \frac{t}{d_h^2 RC}$, $X^* = \frac{x^*}{d_h}$, $Y^* = \frac{y^*}{d_h}$, $N^* = \frac{n^*}{d_h}$, as a result of which equation (11) assumes the form

$$\frac{\partial^2 \theta^*}{\partial X^{*2}} + \frac{\partial^2 \theta^*}{\partial Y^{*2}} = \frac{\partial \theta^*}{\partial Z^*} \quad (14)$$

and the boundary conditions (12) and (13) at the surface Σ^* become

$$\left. \begin{aligned} \frac{\partial \theta^*}{\partial N^*} &= -\frac{1}{4}, \\ \theta^*(X^*, Y^*, 0) &= 0. \end{aligned} \right\} \quad (15)-(16)$$

The reduced potential E_0 on the electrical model may be determined by formulating the energy balance equation for the model:

$$dE_0 = \frac{i_w P^*}{A^* C} dt \quad (17)$$

Integrating from E_0 to E_b and from t_0 to t , we obtain

$$\int_{E_0}^{E_b} dE_b = \int_0^t \frac{i_w P^*}{A^* C} dt \quad (18)$$

or

$$E_b = E_0 \frac{A i_w t}{C d_h^2} \quad (19)$$

or, in dimensionless form,

$$\theta_b^* = Z^* \quad (20)$$

Comparing equation (4) and its boundary conditions (5), (6) with equation (14) and its boundary conditions (15), (16), we note that both systems of equations are identical. Consequently, the solution of one system of equations is a solution of the other system of equations. The boundary condition of constant heat input is replaced by constant influx of current in the electrical model. The present investigation is based on this analogy

EXPERIMENTAL PART

The apparatus was made up of the components shown in figure 2. In order to approximate a constant flow of current in the model at the boundary, it was necessary to divide the current supply into a definite number of dc inputs along the boundary. The method yielding the most satisfactory results is illustrated in figure 3.

For the resistance, we used conducting paper with $R \approx 1400$ ohms per square inch. The resistance of this sheet was linear within 2% in any direction, but it was approximately 10% higher across the sheet than along it. In order to render the resistance of the model uniform in every direction, the models were fabricated from two layers of conducting sheet, cut out so that the cross

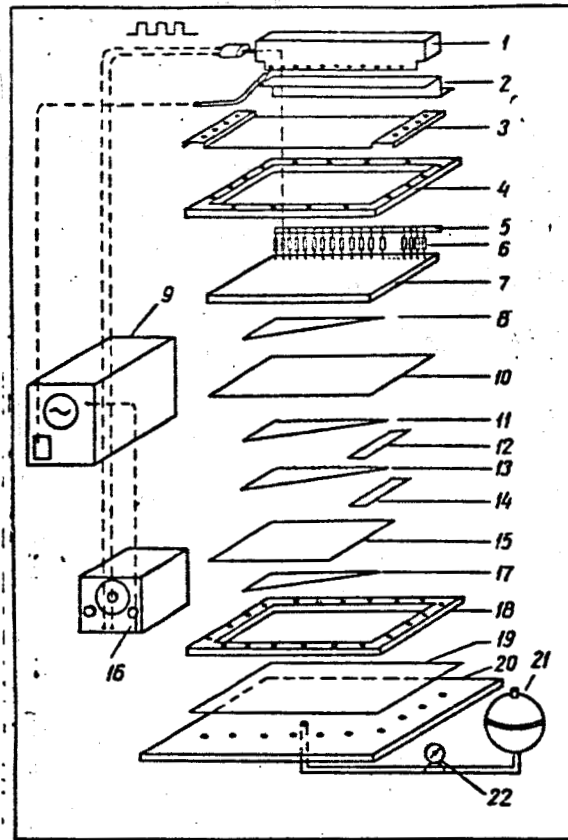


Figure 2. Principal Components of the Apparatus:

1) Protective Shield; 2) Protective Insert; 3) Protective Plate; 4) Flange; 5) Common Busbar; 6) Input Resistances; 7) Measurement Panel; 8) Aluminum Foil; 9) Oscilloscope; 10) Dielectric; 11) Upper Half of Resistance Model; 12) Upper Half of Auxiliary Model; 13) Lower Half of Resistance Model; 14) Lower Half of Auxiliary Model; 15) Dielectric; 16) Square Pulse Generator; 17) Aluminum Foil; 18) Frame; 19) Rubber Insert; 20) Cast Iron Plate; 21) Pressure Tank; 22) Pressure Indicator.

direction of half the model would correspond to the long direction of the 14 other half. When the conducting sides of the paper were joined, the resistance of the models was about 700 ohms per square inch.

To increase the capacitance of the model, the sheets of the dielectric and metal foil were placed on either side of the model made up of the resistances

(fig. 3). As a result, the capacitance of the model was approximately equal to 1000 pF/in^2 .

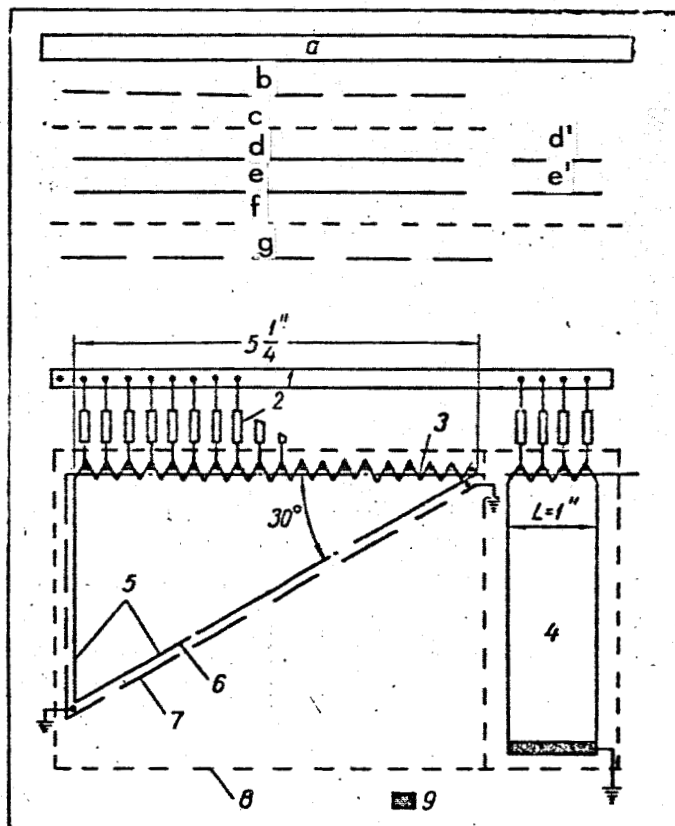


Figure 3. Basic and Auxiliary Models Used to Solve the Problem of a Duct with Cross Section in the Shape of an Equilateral Triangle. The Construction and Layout of These Models are Shown: a) Panel; b) Foil; c) Dielectric; d) Upper Half of Resistance Model; d') Auxiliary Model; e) Lower Half of Resistance Model; e') Auxiliary Model; f) Dielectric; g) Foil. 1) Common Busbar; 2) Input Resistances; 3) Boundary; 4) Auxiliary Model; 5) Adiabatic Lines; 6) Conducting Sheet; 7) Foil; 8) Dielectric; 9) Silver Paint.

Instead of measuring all the parameters required in order to determine the dimensionless potential θ^* and dimensionless time Z^* , we constructed an auxiliary model of conducting sheet, which was joined directly with the sheet from which the main model was cut. The auxiliary model was again cut out of two pieces of conducting sheet situated at right angles to one another.

It is apparent from the analysis that the potential measured at the inputs of the auxiliary model is given by

$$E_{aux} = 4i_w R.$$

Another useful measurement may be performed on the model itself. The slope of the potential as a function of time approaches a constant value as t increases. It follows from the analysis that

$$\left. \frac{dE}{dt} \right|_{t>0} = \frac{4i_w}{C d_h^2} \quad (21)$$

Invoking the dimensionless variables, we obtain

$$\theta^* = \frac{E - E_0}{4i_w R d_h^2} = \frac{E - E_0}{E_{aux} d_h^2}, \quad (22)-(23)$$

$$Z^* = \frac{t}{d_h^2 RC} = \frac{t}{4i_w R d_h^2} \left. \frac{dE}{dt} \right|_{t>0} = \frac{t}{E_{aux} d_h^2} \left. \frac{dE}{dt} \right|_{t>0}$$

Consequently, θ^* and Z^* may be ascertained from measurements of E_0 , E , t , d_h^* , 15
 E_{aux} , and dE/dt .

The frame for the model was constructed so as to protect the model and input resistances from harmful electrical effects without the buildup of added injurious capacitance. A rubber insert held the model and auxiliary model tight with a uniform pressure of approximately seven pounds per square inch when pressure was created in the tank by a bicycle pump. Forty holes 3/16 of an inch in diameter were drilled along the base of the protective cover, so that the oscilloscope probes could be brought in contact with each input resistance. A shielded lead was connected to the busbar for the power supply, which was fed in through the end of the protective cover. The length of the lead-in was three inches and it terminated in a banana jack, which was connected to the output of

a square pulse generator with a resistance of 600 ohms and a voltage of 55 V. 16
 Pertinent data on the construction of the model and the experimental technique
 may be found in reference 5.

COMPARISON OF THE MODEL AND ANALYTICAL SOLUTIONS

The analytical solutions for the wall temperature distributions in creeping flow in circular ducts and between parallel plates with constant heat flux at the wall may be obtained from the solutions given in reference 6 for non-steady-state convection. Transforming these solutions into dimensionless variables, we obtain

$$\theta_w = Z + \frac{1}{48} - \frac{1}{8\pi^2} \sum_{n=1}^{\infty} \frac{\exp(-16n^2\pi^2 Z)}{n^2} \quad (24)$$

for parallel plates and

$$\theta_w = Z + \frac{1}{32} - \frac{1}{4} \sum_{n=1}^{\infty} \frac{\exp(-4B_n^2 Z)}{B_n^2} \quad (25)$$

for circular ducts.

Using up to 35 terms of the series, Zess has computed the dimensionless temperature θ_w at the wall for various positions Z along the duct and for the surfaces of parallel plates. These results are indicated by the solid curves in figure 4, which also gives the previously described experimental data obtained on our apparatus. It is evident from figure 4 that the experimental results are in good agreement with the theoretical data.

SOLUTIONS FOR EQUILATERAL POLYGONS

Measurements were performed using other geometries and employing the same experimental methods. Data on an equilateral triangle are shown in figures 4 and 5. The variation of the dimensionless wall temperature in two positions

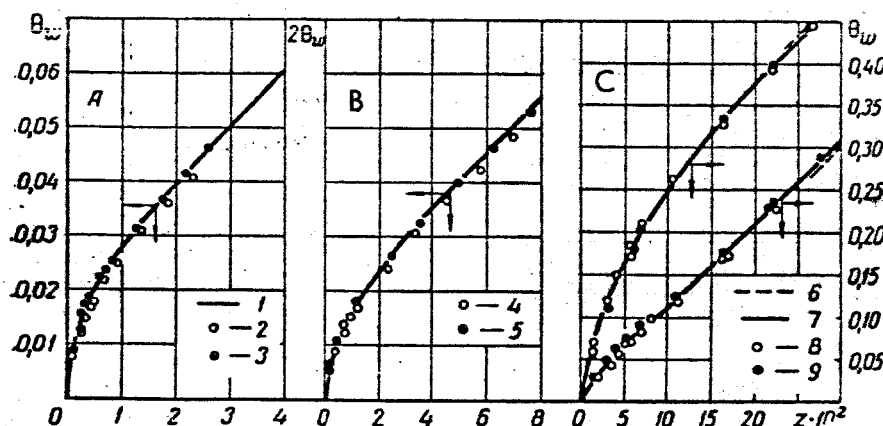


Figure 4. Dimensionless Temperature Distribution at the Wall for Ducts A, B, C (See Table):

- 1) Solution Obtained with Series; 2) Model No. P1; 3) Model No. P2;
- 4) Model No. C1; 5) Model No. C2; 6) Asymptotic Solution of Clayborne; 7) Analog Solution; 8) Model No. T1; 9) Model No. T2.

moving downward along the tube is shown in figure 4. The peripheral wall temperature distributions at various distances from the input are given in figure 17 5.

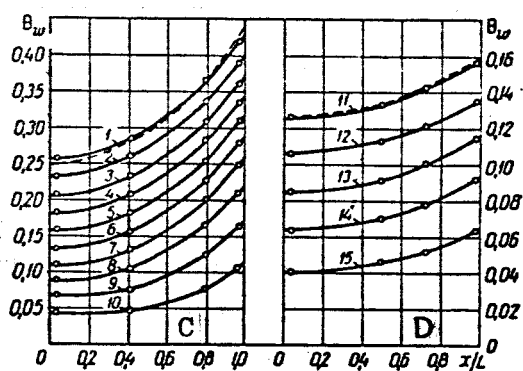


Figure 5. Dimensionless Temperature Distribution at the Wall of Ducts with Cross Sections C and D for Various Values of Z:

- Z = 1) 0.250; 2) 0.225; 3) 0.200; 4) 0.175; 5) 0.150; 6) 0.125;
- 7) 0.100; 8) 0.075; 9) 0.050; 10) 0.025; 11) 0.10; 12) 0.08;
- 13) 0.06; 14) 0.04; 15) 0.02.

The dashed curves in both figures correspond to solutions given in reference 2 for a completely steady flow. The experimental results are again in good agreement with the theoretical data. It is important to note that figure 5 represents a graph of a series of experimental curves analogous to the curves in figure 4.

TABLE
DUCTS OF VARIOUS SHAPES WITH THE BOUNDARY CONDITION $q_w = \text{const}$

Duct	Section	Duct	Section
A		E	
B		F	
C		G	
D			

The wall temperature distributions for squares, pentagons, hexagons, and octagons are given in figures 5 and 6, in correspondence with the table. The dashed curves again correspond to the asymptotic solutions for points far removed from the duct entrance region. These asymptotic solutions are obtained from the solutions for an equilateral polygon with n sides:

$$\theta_w = Z + \frac{1}{32} + \frac{1}{16} \left[\left(\frac{X}{L} \right)^2 - \frac{1}{6} \right] \tan^2 \frac{\pi}{n}, \quad (26)$$

which, to the best of the author's knowledge, has not been published heretofore.

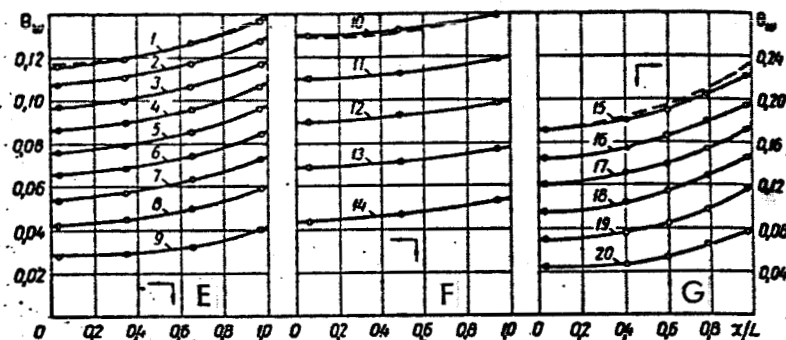


Figure 6. Dimensionless Temperature Distribution at the Wall for Ducts with the Shapes E, F, G for Various Values of Z:

18

Z = 1) 0.09; 2) 0.08; 3) 0.07; 4) 0.06; 5) 0.05; 6) 0.04; 7) 0.03;
8) 0.02; 9) 0.01; 10) 0.10; 11) 0.08; 12) 0.06; 13) 0.04; 15) 0.150;
16) 0.125; 17) 0.100; 18) 0.075; 19) 0.050; 20) 0.025.

SUMMARY OF NOMENCLATURE

A = cross sectional area of duct; A^* = surface area of electrical model;
 B_n = positive roots of the equation $J_1(B) = 0$; c = specific heat; C = capacitance of model per unit area; d_h = hydraulic diameter of duct; d_h^* = hydraulic diameter of electrical model; E = potential at any point on the electrical model; E_{aux} = potential at the input to the auxiliary model; i_w = electric current in the model per unit length along the boundary; J_1 = first-order Bessel function; k = coefficient of thermal conductivity; n = distance perpendicular to the duct wall; n^* = distance perpendicular to the boundary of the electrical model; N = dimensionless distance normal to the duct wall, $N = n/d_h$; N^* = dimensionless distance normal to the boundary of the electrical model, $N^* = n^*/d_h^*$; P = duct perimeter; P^* = perimeter of the electrical model; Pr = Prandtl number, $Pr = \nu/a$; q_w = heat flux of fluid per unit cross sectional area of duct; R = resistance of conducting sheet; Re = Reynolds number, $Re = ud_h/\nu$; t = time; T = temperature; w = velocity of fluid in z-direction; x, y, z = coordinates in the

investigated thermal system; x^* , y^* = coordinates of electrical analog model; X , Y , Z = dimensionless coordinates of thermal system, $X = x/d_h$, $Y = y/d_h$, $Z = z/d_h RePr$; X^* , Y^* , Z^* = dimensionless coordinates in electrical analog model, $X^* = x^*/d_h^*$, $Y^* = y^*/d_h^*$, $Z^* = t/d_h^{*2} RC$; a = thermal diffusivity, $a = k/\rho c$; θ = dimensionless temperature, $\theta = (T - T_0)k/4q_w d_h$; θ^* = dimensionless potential, $\theta^* = (E - E_0)/4i_w d_h^* R$; ρ = density; σ = inside surface of duct; σ^* = curve corresponding to the boundary of the electrical analog model; Σ = dimensionless form of curve σ ; Σ^* = dimensionless form of curve σ^* . Subscripts: b) reduced, or average; w) wall, or boundary; 0) condition at $z = 0$ or $t = 0$.

REFERENCES

1. Lyon, R. N. Oak Ridge National Laboratory Report 361, 1949.
2. Clayborne, H. C. Oak Ridge National Laboratory Report 985, 1951.
3. Hartnett, J. P. and T. F. Irvine, Jr. J. Am. Inst. Chem. Engrs., Vol. 3, 1957.
4. Fatt, I. J. Am. Inst. Chem. Engrs., Vol. 4, 1958.
5. Pearson, J. T. M. S. Thesis, North Carolina State College, 1961.
6. Siegel, R. Trans. ASME, Vol. 81, 1959.

6 March 1963

New York University

Translated for NASA by Stemar Engineering, Inc.
4940 Long Beach Blvd., Long Beach, California